Bulletin of the Seismological Society of America, Vol. 99, No. 3, pp. 1746–1759, June 2009, doi: 10.1785/0120080305

The 1911 M ~6.6 Calaveras Earthquake: Source Parameters and the Role of Static, Viscoelastic, and Dynamic Coulomb Stress Changes Imparted by the 1906 San Francisco Earthquake

by Diane I. Doser, Kim B. Olsen, Fred F. Pollitz, Ross S. Stein, and Shinji Toda*

Abstract The occurrence of a right-lateral strike-slip earthquake in 1911 is inconsistent with the calculated 0.2–2.5 bar static stress decrease imparted by the 1906 rupture at that location on the Calaveras fault, and 5 yr of calculated post-1906 viscoelastic rebound does little to reload the fault. We have used all available first-motion, body-wave, and surface-wave data to explore possible focal mechanisms for the 1911 earthquake. We find that the event was most likely a right-lateral strike-slip event on the Calaveras fault, larger than, but otherwise resembling, the 1984 M_w 6.1 Morgan Hill earthquake in roughly the same location. Unfortunately, we could recover no unambiguous surface fault offset or geodetic strain data to corroborate the seismic analysis despite an exhaustive archival search. We calculated the static and dynamic Coulomb stress changes for three 1906 source models to understand stress transfer to the 1911 site. In contrast to the static stress shadow, the peak dynamic Coulomb stress imparted by the 1906 rupture promoted failure at the site of the 1911 earthquake by 1.4–5.8 bar. Perhaps because the sample is small and the aftershocks are poorly located, we find no correlation of 1906 aftershock frequency or magnitude with the peak dynamic stress, although all aftershocks sustained a calculated dynamic stress of $\geq$3 bar. Just 20 km to the south of the 1911 epicenter, we find that surface creep of the Calaveras fault at Hollister paused for ~17 yr after 1906, about the expected delay for the calculated static stress drop imparted by the 1906 earthquake when San Andreas fault postseismic creep and viscoelastic relaxation are included. Thus, the 1911 earthquake may have been promoted by the transient dynamic stresses, while Calaveras fault creep 20 km to the south appears to have been inhibited by the static stress changes.

Introduction

The 1906 San Francisco earthquake is calculated to have reduced the static stress along adjacent, subparallel, strike-slip faults in the greater San Francisco Bay area (Fig. 1) (Simpson and Reasenberg, 1994; Harris and Simpson, 1998). Although questioned by Felzer and Brodsky (2005), the 1906 stress shadow has been invoked by Simpson and Reasenberg (1994), Harris and Simpson (1998), Stein (1999), and Pollitz *et al.* (2004) to explain the roughly order-of-magnitude drop in the rate of $M \geq 6$ shocks in the Bay area in the 75 yr following the 1906 earthquake. In contrast to 14 such events in the 75 yr preceding 1906, only one $M_w \geq 6$ event, the 1911 Calaveras earthquake, struck in the 75 yr after the 1906 earthquake. At least three studies (Jaumé and Sykes, 1996; Harris and Simpson, 1998; Hori and Kaneda, 2001) analyzed why the 1911 earthquake could have occurred in the 1906 stress shadow. Harris and Simpson (1998) and Hori and Kaneda (2001) argued that the 1906 earthquake might have delayed the 1911 event by up to 5 yr, either because it was about to rupture in 1906 or because of the high Calaveras fault creep rate. Jaumé and Sykes (1996) argued that the 1911 event could have struck on a thrust fault oriented parallel to the Calaveras fault, in which case the 1906 stress changes would be positive, promoting failure. It is thus necessary to determine the focal mechanism, location, and magnitude of the 1911 event because the sign and magnitude of stress change are dependent on the geometry, location, and rake of the receiver fault (Simpson and Reasenberg, 1994).

Here, we use first-motion, regional, and teleseismic waveforms of the 1911 event to determine its focal mechanism

*Order of authorship is alphabetical.

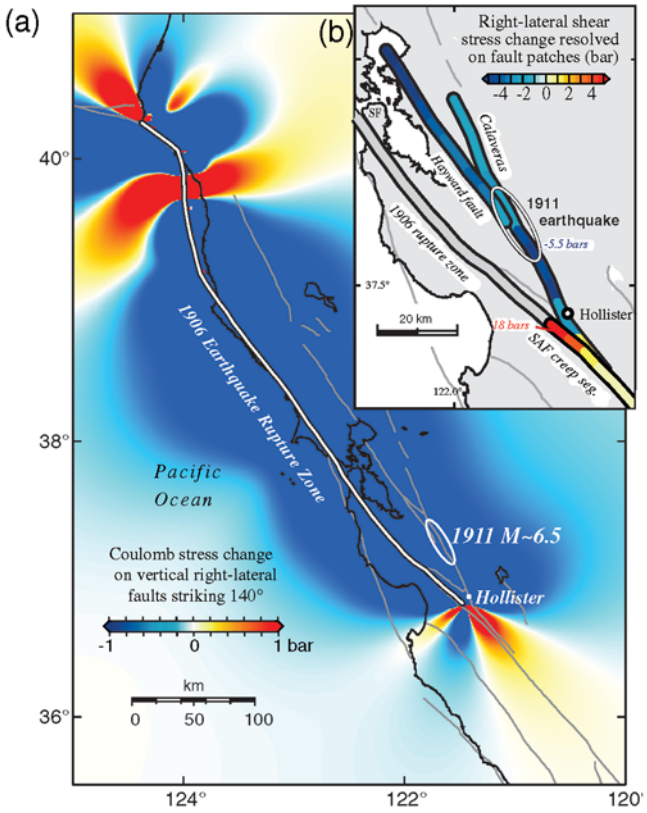

Figure 1. (a) Map showing static Coulomb stress change imparted by the 1906 earthquake (using the coseismic slip model of Thatcher *et al.*, 1997) on vertical right-lateral strike-slip faults striking 140°, the average northern San Andreas strike. (b) Right-lateral shear stress change resolved on the local strike of the Hayward and Calaveras faults and creeping segment of the San Andreas fault (SAF).

and improve its magnitude estimation. We then resolve the static and dynamic stress changes imparted by the 1906 shock on the fault plane interpreted from this mechanism. Our conclusions are tempered by the limited low-quality seismic data but suggest that the event was right lateral and most likely struck on the Calaveras fault.

Previous Studies

The initial studies of the 1911 Calaveras earthquake summarized mainshock and aftershock arrival times (Wood, 1912a), intensities (Templeton, 1911), earthquake damage, and instrumental and human perceptions (Oldenbach, 1911). No reports of surface faulting accompanied the earthquake, although damage reports were later interpreted to indicate a rupture on the Calaveras fault. Gutenberg and Richter (1954) assigned the event a magnitude of 6.6, and Ellsworth (1990) assigned an M_S of 6.5.

Oppenheimer *et al.* (1990) used Wood's travel times to relocate the 1911 aftershocks under the assumption that they occurred along the Calaveras fault, concluding that the 1911 aftershocks occurred on same section of the Calaveras fault as the aftershocks of the 24 April 1984 M 6.1 Morgan Hill mainshock. By comparing intensities for the 1984 and 1911 events, Toppozada (1984) concluded that both events had the same magnitude and occurred on overlapping segments of the Calaveras fault. Bakun (1999) reanalyzed the intensity data and found it to be consistent with Calaveras fault rupture in a location similar to that of the 1984 mainshock. He estimated a moment magnitude (M_w) of 6.2 (+0.2, −0.3 units) for the mainshock.

Seismic Analysis

In an attempt to improve the constraints on the focal mechanism and magnitude of the 1911 mainshock, we collected first-motion information from instrumental records and from the literature and obtained all still-extant seismograms for the event. Sadly, nearly all observations from the numerous Jesuit seismic observatories in the United States have been lost. But fortuitously, we were able to obtain seismograms at two stations that recorded both the 1911 and 1984 events. In one case (Göttingen) the seismograms were recorded by instruments that had very similar responses in 1911 and 1984 (Table 1).

Table 1

Instrument Response Information

Instrument	Seismometer Period (sec)	Damping Ratio	Magnification
GTT north–south (1911) astatic pendulum	12.2	4:1	160
GTT east–west (1911) astatic pendulum	12.2	3.5:1	159
GTT north–south (1984) astatic pendulum	9.4	2.8:1	153
GTT east–west (1984) astatic pendulum	10.3	3.5:1	157
DBN east–west (1911) Wiechert	5	4:1	170
DBN north–south (1911) Wiechert	5	4:1	170
DBN east–west (1984) Galitzin	25	—	310
DBN north–south (1984) Galitzin	25	—	310
OTT north–south (1911) Bosch	5.6	8:1	120
OTT east–west (1911) Bosch	8	8:1	120
SLM north–south (1911) Wiechert	8	5:1	200
SLM east–west (1911) Wiechert	8	5:1	200

Abbreviations: Göttingen, GTT; Debilt, DBN; Ottawa, OTT; St. Louis, Missouri, SLM.

First Motions

P waves for the 1911 mainshock were visible only at stations located in central California (Fig. 2). The record for the Los Gatos (GAT) seismoscope is published in Oldenbach (1911). First motions for Mt. Hamilton (MHC) and Santa Clara (SCL) were read from copies of the original seismograms. Seismograms at MHC indicated the ground moved down, east and south during the mainshock, contrary to Wood's (1912b) observation that indicated west and north first motions. Ground motion information for Berkeley (BRK) was obtained from Wood (1912b).

To examine the effects of station azimuths and takeoff angles on the focal mechanism, we considered two possible epicenters: a location similar to the Morgan Hill earthquake (37.31° N, 121.68° W) (dots, Fig. 2) and the intensity center of Bakun (1999) (37.39° N, 121.8° W) (stars, Fig. 2). Figure 2 compares the first-motion data to the strike-slip mechanism of the 1984 Morgan Hill earthquake (solid lines) and representative normal and reverse focal mechanisms (dashed lines) for earthquakes located just west of the Calaveras fault

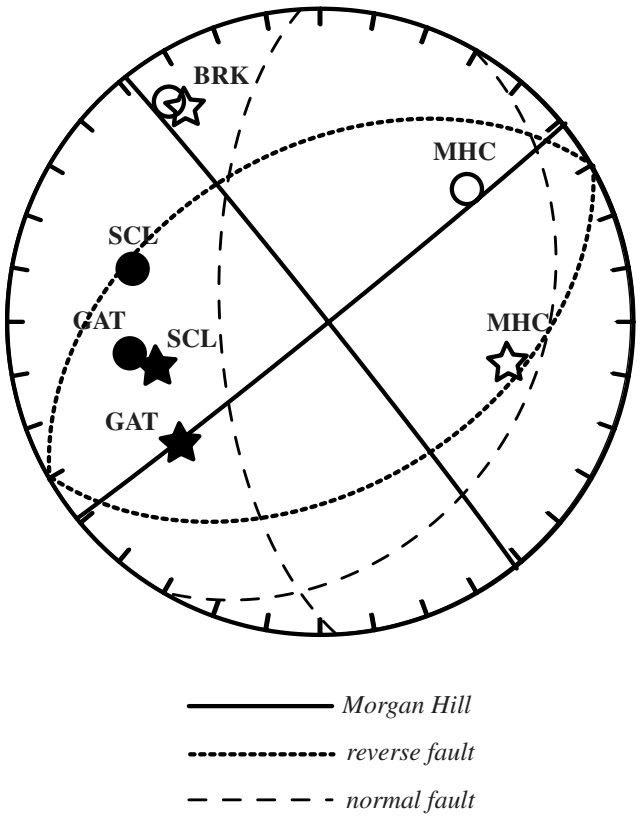

Figure 2. First motions observed for the 1911 Calaveras earthquake. Open symbols are dilatations; solid symbols are compressions. Dots indicate azimuth and takeoff angle positions using the 1984 Morgan Hill epicenter; stars indicate positions using Bakun's (1999) intensity center. Focal mechanisms shown are for the Morgan Hill earthquake (solid lines) and representative normal and reverse mechanisms (dashed and dotted lines, respectively) for earthquakes occurring in this region of the Calaveras fault (Manaker *et al.*, 2005).

from Manaker *et al.* (2005). It appears the data are most consistent with the strike-slip or normal mechanisms, but they are not sufficient to adequately distinguish between mechanisms.

Body Waves

Few instruments with sufficient gain to record a magnitude 6.0–6.5 earthquake were operating in the world in 1911. After an extensive search of seismogram archives in the United States and requests to seismograph stations operating elsewhere in the world, we were able to obtain *S* waveforms recorded at St. Louis, Missouri (SLM, $\Delta = 25°$), Göttingen (GTT, $\Delta = 82°$), Debilt (DBN, $\Delta = 80°$), and Ottawa (OTT, $\Delta = 35°$). In contrast, no *S* waves were observed at either GTT or DBN for the 1984 Morgan Hill earthquake. We modeled waveforms with the technique of Baker and Doser (1988), modified by Doser and VanDusen (1996). Simple crustal velocity models were used at the source (30 km thick crust with $V_P = 6.3$ km/sec and $V_S = 3.6$ km/sec over a mantle with $V_P = 8.0$ km/sec and $V_S = 4.2$ km/sec) and receivers (35 km thick crust with the same velocities as the source model). The forward modeling indicates that the *SH*-waveform shapes, amplitudes, and polarities match the synthetic seismograms for a strike-slip mechanism similar to the 1984 Morgan Hill earthquake (strike = 320°, dip = 88°, and rake = 178°) (Fig. 3) better than a reverse mechanism (strike = 60°, dip = 45°, and rake = 90°) or a normal mechanism (strike = 30°, dip = 30°, and rake = −60°) with orientations similar to seismogenic structures observed just west of the Calaveras fault (Manaker *et al.*, 2005). For the strike-slip and reverse mechanisms a starting model with M_w of 6.6 best fit the observed seismograms; however, for the normal mechanism a starting model with M_w of 6.4 still over predicted amplitudes observed at European stations (Fig. 3).

Surface Waves

Figure 4 shows scanned copies of the original surface waveforms recorded at DBN and GTT in 1911 and 1984. The seismograms have been aligned relative to one another based on event travel times. The seismograms at GTT (Fig. 4a) were recorded with nearly identical instruments (Table 1). Note the similarities in waveform shape between the two events, although the amplitudes for the 1911 waveforms are a factor of ≈5 larger. Waveforms for the 1911 and 1984 earthquakes recorded at DBN also show similar characteristics (Fig. 4b), although instrument responses differ (Table 1).

Static Coulomb Stress and Boundary-Element Analysis

We calculate that the 1906 earthquake imparted a 2–4 bar left-lateral static shear stress change and a 0.2–2.5 bar drop in Coulomb stress on the Calaveras fault

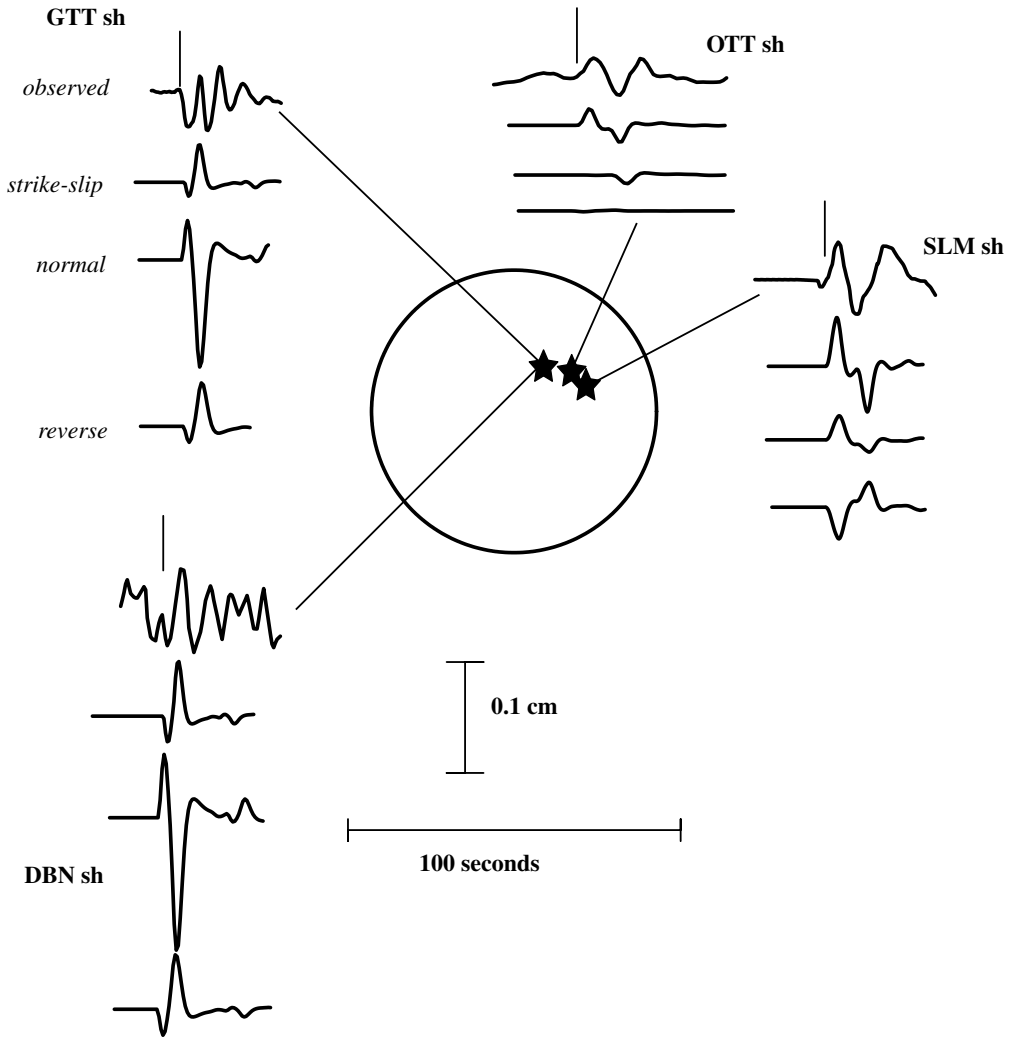

Figure 3. Results of waveform modeling. The top seismogram of each group is observed, the second seismogram is synthetic for right-lateral strike-slip mechanism similar to the 1984 Morgan Hill earthquake, the third seismogram is synthetic for normal mechanism, and the fourth seismogram is synthetic for reverse mechanism (see text for details). Solid vertical lines indicate the beginning of the *SH* phase on the observed seismogram.

at the site of the future 1911 earthquake (Fig. 5). We use the Wald *et al.* (1993), Thatcher *et al.* (1997), and Song *et al.* (2008) source models for the 1906 earthquake in an elastic half-space (Fig. 6). The Wald *et al.* (1993) slip model, in part constrained by seismic records from the earthquake, contains a concentration of slip in Sonoma and southern Mendocino Counties as well as on the San Francisco Peninsula and into southern Marin County toward the north (Fig. 6). In contrast, the Thatcher *et al.* (1997) and Song *et al.* (2008) models are smoother, with significant slip from Point Arena to the north and Hollister (Fig. 5) to the south. The geodetic data used in the Thatcher *et al.* (1997) and Song *et al.* (2008) models requires greater 1906 slip on the San Andreas fault near the 1911 epicenter than in the Wald *et al.* (1993) model, making them more reliable for Calaveras fault calculations. The slip profiles shown in Figure 6 were extended to the bottom of the vertical fault plane (12 km for the Wald *et al.* [1993] and Song *et al.* [2008] models and 10 km for the Thatcher *et al.* [1997] model). The Thatcher *et al.* (1997) (−1.9 bar) and Song *et al.* (2008) (2.5 bar) models yield the largest decreases; the Wald *et al.* (1993) model (−0.2 bar) is the smallest (Fig. 5). Harris and Simpson (1998) calculated a 2.0 bar stress change, and most studies find measurable seismicity responses to stress changes exceeding 0.1 bar (Stein, 1999). Hollister (Figs. 1b and 5), whose 100 yr surface creep record is used for this study, has a static Coulomb stress drop of 5.8 bar for the Thatcher *et al.* (1997) model, 6.6 bar for the Song *et al.* (2008) model, and 2.3 bar for the Wald *et al.* (1993) model.

Estimating the Earthquake Delay Caused by the 1906 Stress Shadow

We next performed a boundary-element analysis to estimate the amount of tectonic stress accumulation that would

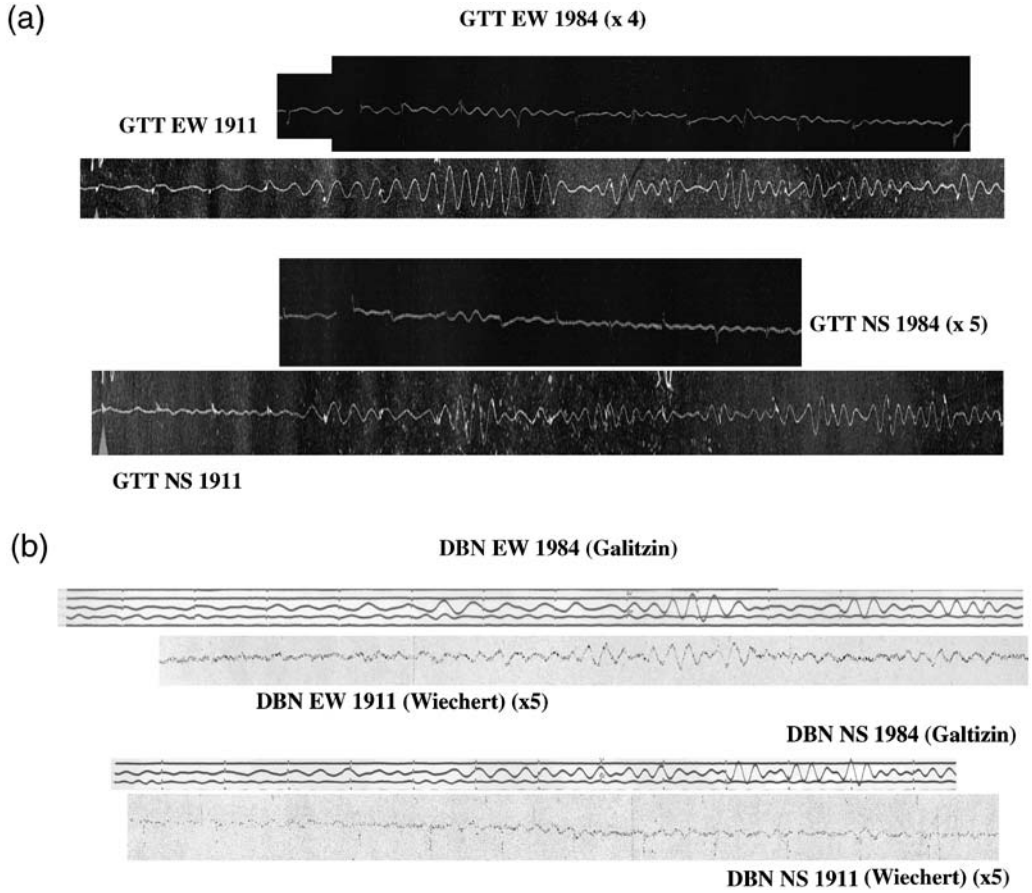

Figure 4. Comparison of surface waves recorded at (a) GTT and (b) DBN from scanned copies of the original seismograms. The seismograms are aligned with each other based on earthquake travel times. The horizontal scales have been adjusted so that the seismograms have the same time scale. For visibility the 1984 seismograms at GTT have been enlarged by the amounts shown, although the instrument responses in 1911 and 1984 (Table 1) are similar. For DBN the 1911 seismograms have been enlarged for visibility because they are recorded on instruments with much lower gains than the 1984 seismograms (see Table 1).

be needed to shed the 0.2–2.5 bar stress imposed by the 1906 earthquake. Here we treat the Calaveras fault as a 15 km deep surface of freely slipping boundary elements, in a manner similar to Toda and Stein (2002). The amount of stress depends not just on the magnitude of the stress change at the 1911 site and the long-term slip rate but also on the geometry and distribution of stresses along the entire fault because the longer and straighter the fault, the more it will slip in response to a given change in stress. We find that 350 ± 50 mm of left-lateral slip (also known as backslip) would be needed to relieve the imposed stress (Fig. 7). Given the long-term 15 ± 3 mm/yr slip rate on this section of the Calaveras fault (Wills *et al.*, 2008), the slip deficit would be removed in 23.3 ± 0.25 yr. Instead, the 1911 earthquake struck after just 5 yr, long before the stress drop imparted by the 1906 shock is likely to have been erased by stress accumulation.

The ratio of the 1906 stress drop on the Calaveras fault to its long-term stressing rate furnishes a complementary way to estimate the expected delay of $M_w \sim 6$ Calaveras fault earthquakes. The stressing rate is influenced by the stress contribution from other faults within about 30 km of the 1911 site (e.g., 2–3 fault depths), such as the southern Hayward and San Andreas faults. So we used an interseismic stressing model in which locked faults are treated as virtual dislocations (they are slipped backwards at their long-term rates) over their locked width in an elastic half-space. We then sample the average stressing rate on the 1911 site on the Calaveras fault over 0–10 km depth (the 1984 Morgan Hill mainshock nucleated at 8 km depth) and find the Calaveras fault stressing rate at the site of the 1911 shock to be 0.15 ± 0.05 bar/yr, the value used by Harris and Simpson (1998). In comparison, Pollitz *et al.* (2004) and Parsons (2006) used 0.09 bar/yr for the Calaveras fault in the absence of creep. The expected delay using our stressing rate then comes to 27 ± 9 yr, in agreement with the boundary-element calculation.

A third way to estimate the delay is to consider the 1911 and 1984 earthquakes as ruptures of the same fault patch. In the absence of the stress changes imparted to the Calaveras fault by the 1906 shock, given the 15 ± 3 mm/yr Calaveras fault slip rate, the period between 1911 and 1984 would nominally accumulate a 1.1 ± 0.2 m

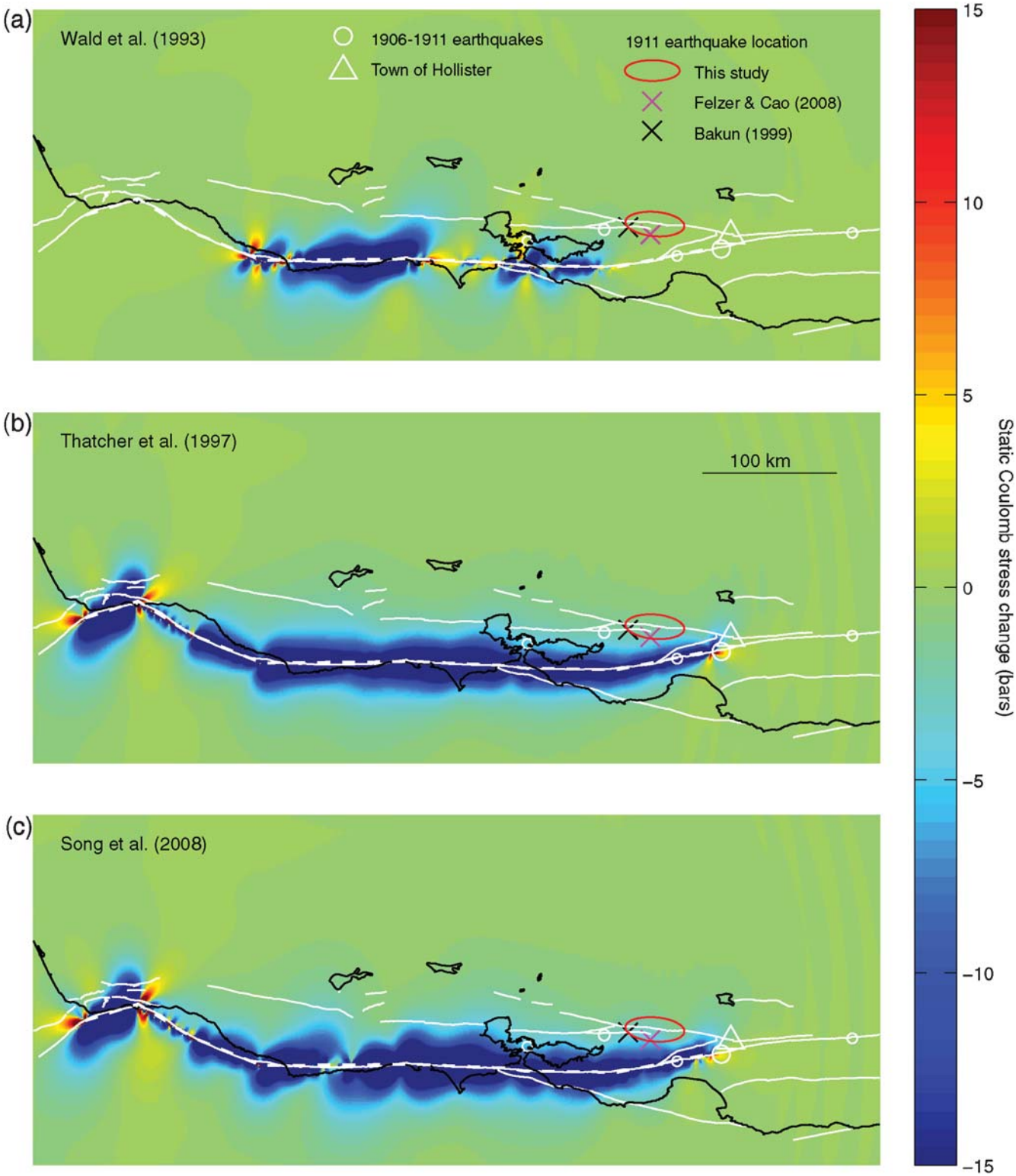

Figure 5. The static Coulomb stress at 8 km depth imparted by the 1906 earthquake using slip models by (a) Wald *et al.* (1993), (b) Thatcher *et al.* (1997), and (c) Song *et al.* (2008), assuming a 0.4 friction coefficient on vertical receiver faults striking 144°. The circle size is proportional to magnitude for the 1906–1911 aftershocks from Meltzner and Wald (2003). (a) Locations for the 1911 earthquake from Bakun (1999) and Felzer and Cao (2008) are indicated X's. The oval indicates the epicentral area we considered in this study.

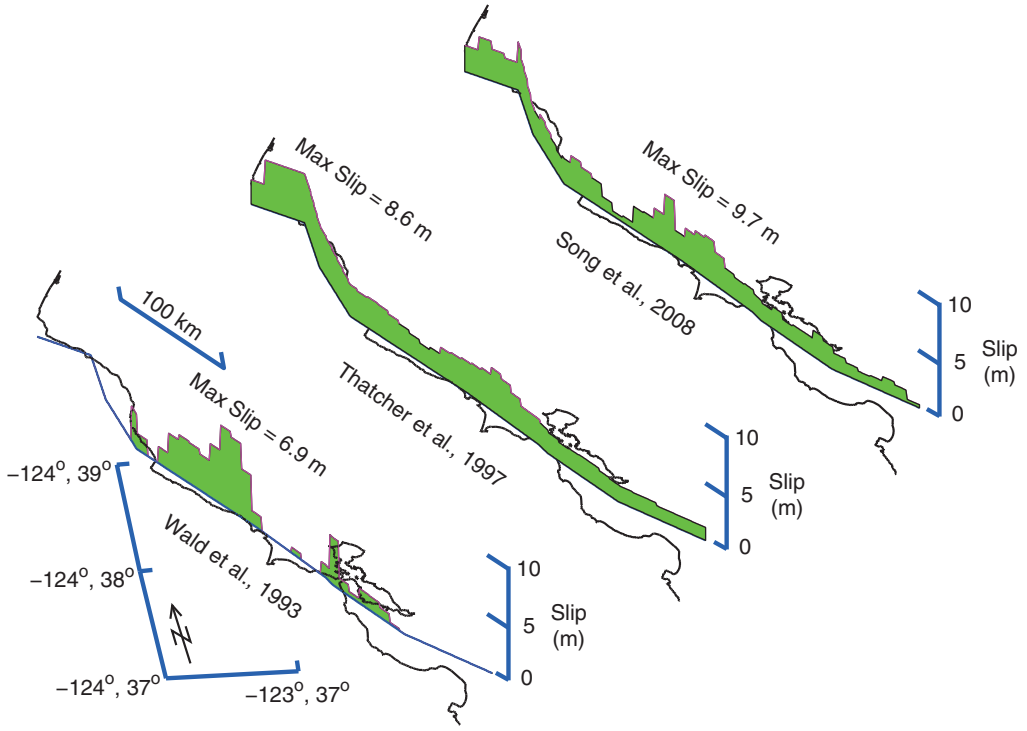

Figure 6. Comparison of the slip models for the 1906 event by Wald *et al.* (1993), Thatcher *et al.* (1997), and Song *et al.* (2008).

slip deficit. A strike-slip M_w 6.5 shock has a typical slip of 1.0 m and a rupture area of 10×30 km (Wells and Coppersmith, 1994). The 1911 aftershock zone as relocated by Oppenheimer *et al.* (1990) is about 20 km long, and the aftershocks of the 1984 Morgan Hill shock extended for ~28 km, with slip occurring over a patchy region of total area 27×11 km (Oppenheimer *et al.*, 1990), in fair agreement with the magnitude estimate provided by our seismic analysis assuming a 3×10^{11} dyne/cm^2 shear modulus. Thus, a minimum interevent time of 73 yr for the 1911 event is needed to reaccumulate sufficient stress for another M_w ~6 shock. If one assumes that the 1911 and 1984 events have typical 30 bar stress drops, then a 4 bar stress drop in 1906 represents about 15% of the total, which would have erased at least 10 yr of stress accumulation, providing a lower bound on the other estimates we have made. But the 1911 and 1984 shocks could have slipped adjacent or complementary patches of the fault, as occurred during the 1934, 1966, and 2004 Parkfield shocks (Segall and Du, 1993; Murray and Langbein, 2006), in which case the interevent time for the 1911 event could be much longer than 73 yr, and the retardation could similarly be much longer than 10 yr.

Dynamic Coulomb Stress Analysis

While the static Coulomb Failure Function (static CFF) for numerous earthquakes has been successfully correlated with aftershocks and subsequent mainshocks, Kilb *et al.* (2002) and Kilb (2003) proposed an alternative parameter to estimate seismic triggering potential, the peak dynamic CFF change, which is highly sensitive to rupture effects such as directivity. They illustrated this sensitivity by an improved correlation of peak dynamic CFF with aftershocks for the M_w 7.3 Landers, California, earthquake, as compared to static CFF estimates. In contrast, static CFF estimates are primarily sensitive to the slip distribution and geometry of the rupture surface.

Here we compare the peak dynamic Coulomb stress changes for the three source models of the 1906 earthquake (Fig. 8). Although Thatcher *et al.* (1997) presented a static displacement model, we use it to generate a kinematic rupture model by assuming an epicenter 10 km south of the Golden Gate off Daly City and a uniform rupture velocity of 2.7 km/sec (as used by Wald *et al.* [1993] for their rupture model of the 1906 event, based on studies of other California strike-slip earthquakes). The Coulomb stress changes were computed at an 8 km depth in a layered regional model within a 630×260 km area using a fourth-order finite-difference method (Olsen, 1994) and a friction coefficient of 0.4 (Stein, 1999) and resolved onto vertical faults parallel to the local strike of the Calaveras fault (144°). Reducing the friction to 0.2 has little effect (Fig. 9). The Wald *et al.* (1993) and Thatcher *et al.* (1997) source models were implemented using a constant (subshear) rupture velocity of 2.7 km/sec, as used in the teleseismic modeling of the Wald *et al.* (1993) study. The Song *et al.* (2008) model, on the other hand, used four different rupture velocities

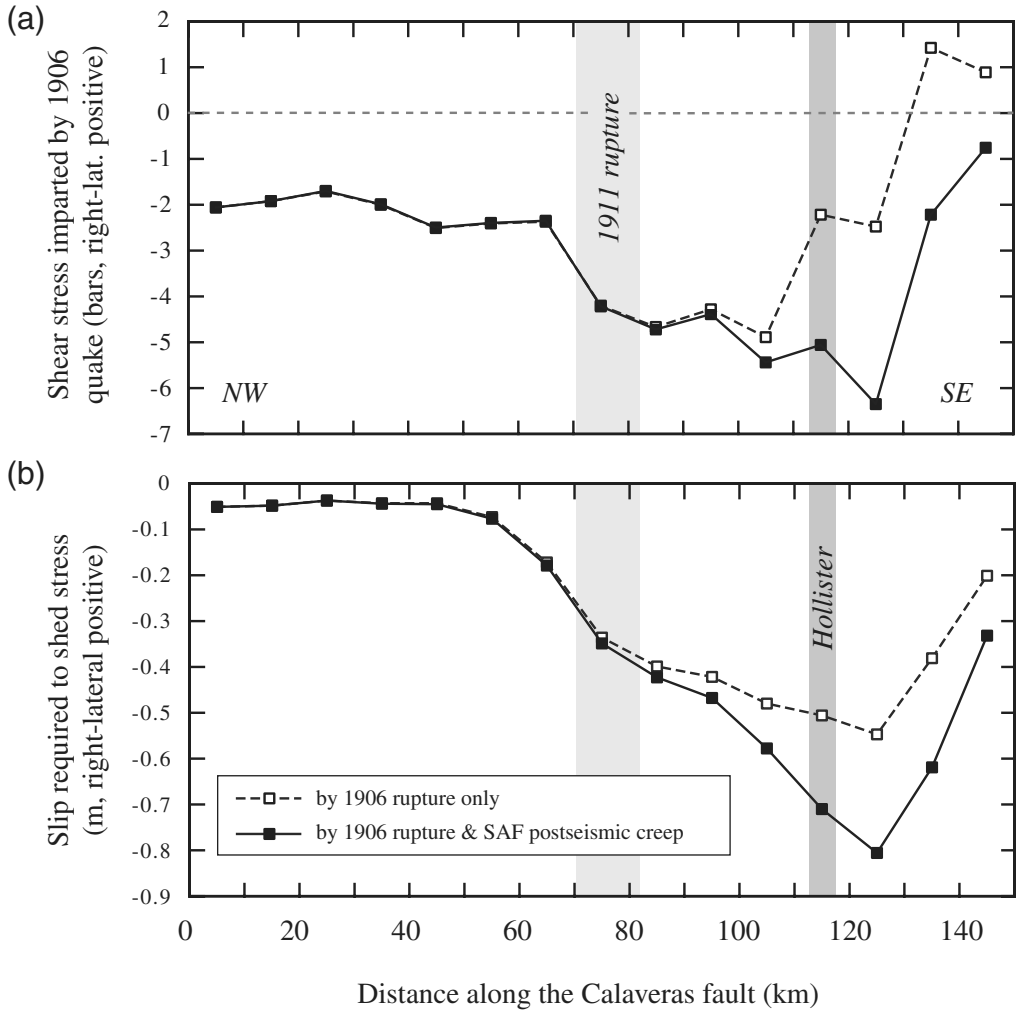

Figure 7. (a) Shear stress imposed by 1906 earthquake on the Calaveras fault, using the Thatcher *et al.* (1997) slip model; the shear stress changes are also shown by colors in Figure 1b. (b) Slip required to shed (or remove) the stress imposed by 1906 earthquake.

along the fault, with a supershear segment located near the epicenter.

The peak dynamic CFF distributions shown in Figure 8 for the three source models reveal more strikingly different patterns. Unlike the static CFF, the peak dynamic CFF are positive everywhere and contain significant effects of the rupture propagation, as pointed out by Kilb (2003), with a strong directivity pattern. The most prominent directivity effects occur for the relatively large slip in the Thatcher *et al.* (1997) and Song *et al.* (2008) models toward the north. In contrast, the peak dynamic CFF values are relatively modest in the epicentral area. The Song *et al.* (2008) model contains smaller peak dynamic CFF values near the epicenter, to a large extent an effect of the supershear rupture velocity in this area. At the site of the 1911 earthquake, the peak dynamic CFFs predicted by the Wald *et al.* (1993), Thatcher *et al.* (1997), and Song *et al.* (2008) models reach ~1, 6, and 6 bar, respectively. The San Andreas fault at Hollister is calculated to have sustained a peak dynamic CFF of 2 bar for the Wald *et al.* (1993) 1906 model and 10 bar for both the Thatcher *et al.* (1997) and Song *et al.* (2008) models. Because the fault is creeping at this locality, it might have been expected to undergo accelerated creep rather than the observed creep pause.

The 1911 earthquake could have been triggered by dynamic Coulomb stresses. In addition to our calculations for the site of the Calaveras shock, we note that the five aftershocks that occurred between the 1906 mainshock and the 1911 earthquake (Meltzner and Wald, 2003) all struck where the dynamic Coulomb stress exceeded 3 bar (Fig. 10). Nevertheless, this test is less stringent than for the static stress change because the peak dynamic stress changes are positive, whereas static stress changes are both positive and negative. Further, aftershocks were not recorded—or did not occur—in many of the regions with the highest peak dynamic stress changes, and as a result there is no correlation between peak dynamic Coulomb stress and either aftershock frequency or magnitude (Fig. 10). The absence of a

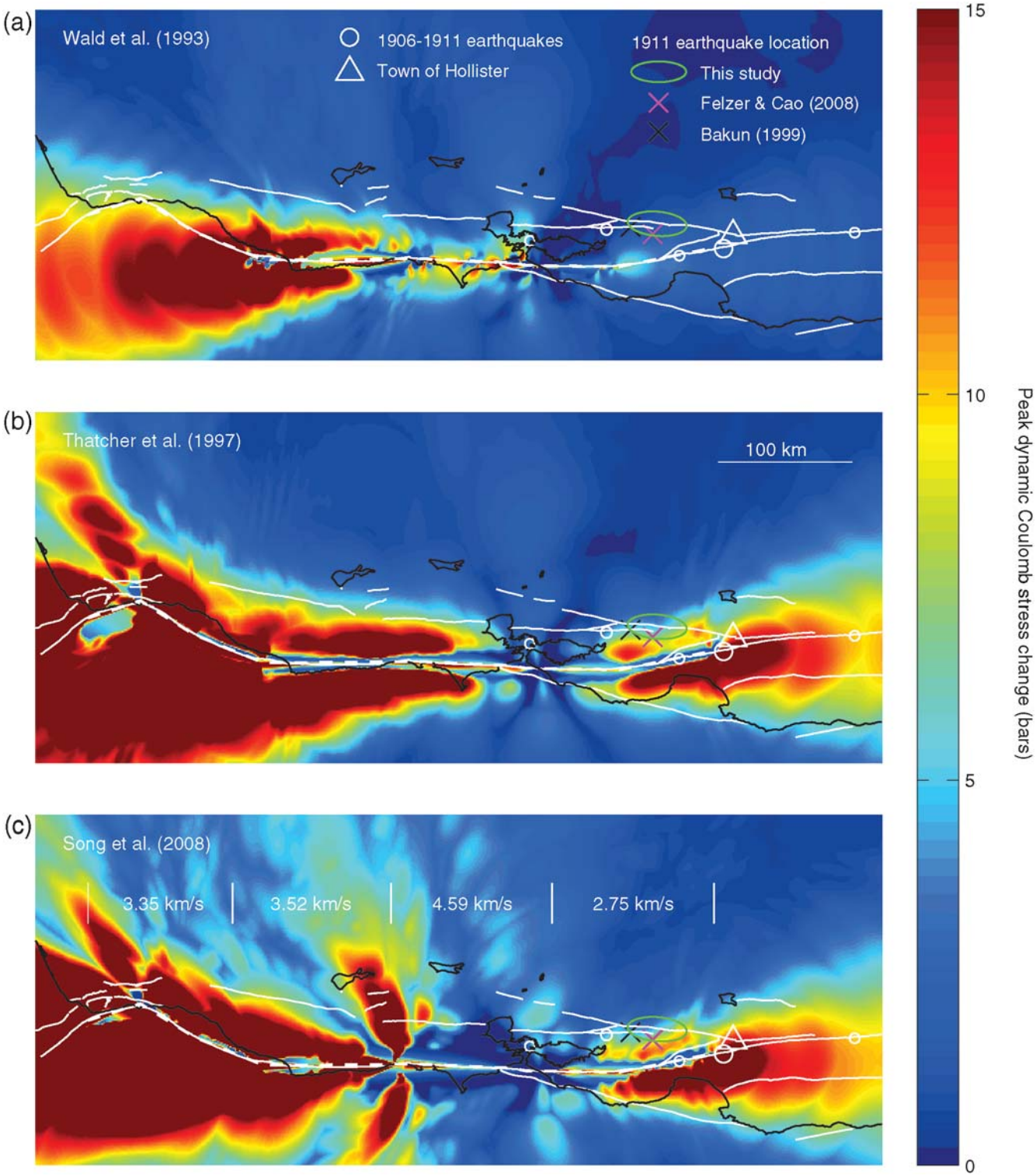

Figure 8. Peak dynamic Coulomb stress distributions generated by the (a) Wald *et al.* (1993), (b) Thatcher *et al.* (1997), and (c) Song *et al.* (2008) source models. The circle size is proportional to magnitude for the 1906–1911 aftershocks from Meltzner and Wald (2003). The spatially variable rupture speed is shown for each model. Receiver fault friction is assumed to be 0.4, and symbols are as in Figure 5. Note that the stress scale ranges over 0–15 bar; blue does not represent a stress decrease as it does in Figure 6.

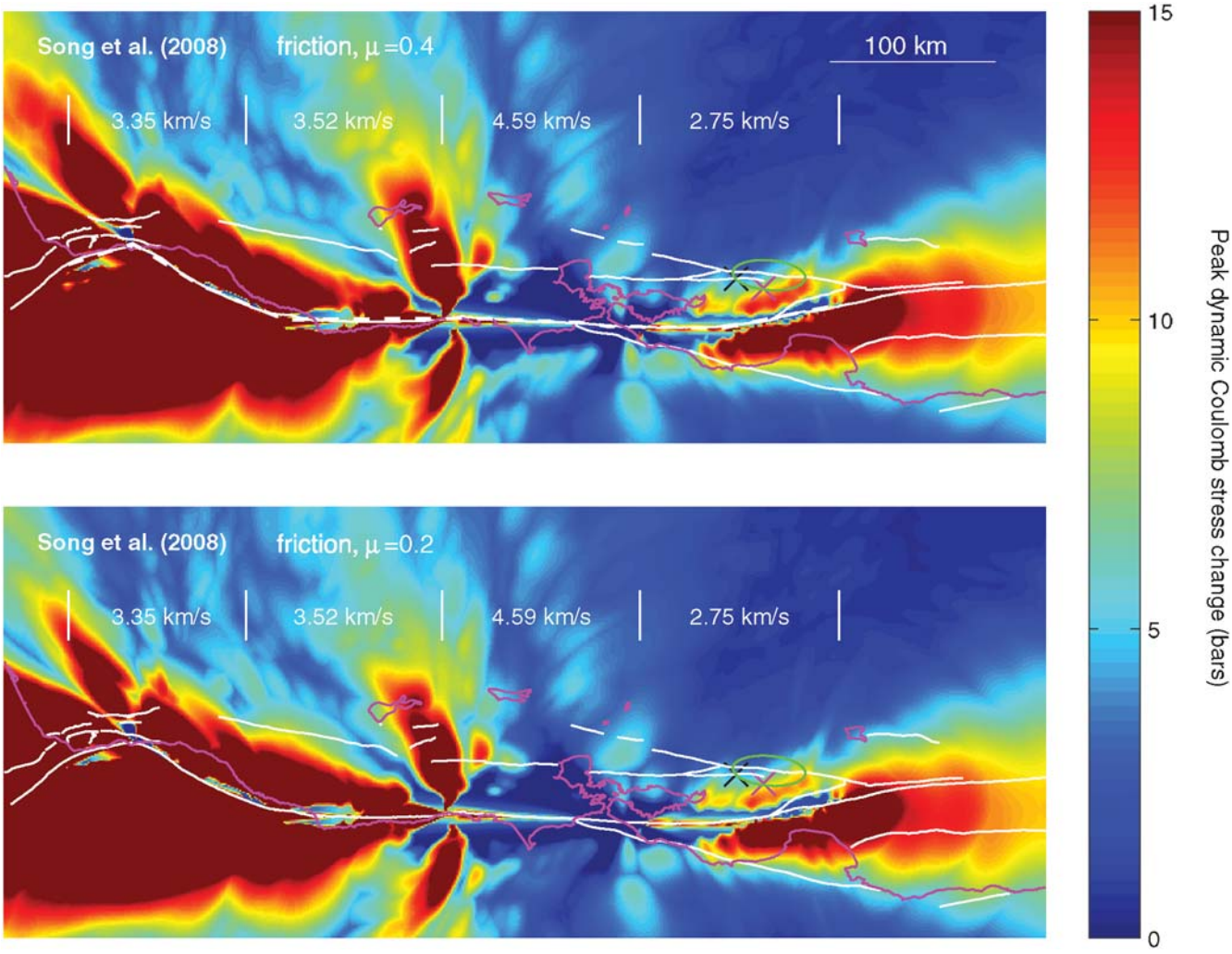

Figure 9. The effect on the peak dynamic Coulomb stress of lowering the assumed friction coefficient on receiver faults from 0.6 (Fig. 8) to 0.4 and 0.2 here is modest.

correlation may be the product of the impoverished aftershock catalog.

Discussion

Inferences on the 1911 Rupture Propagation Direction

The limited seismic data suggest that the mechanism of the 1911 earthquake may be consistent with right-lateral rupture along the Calaveras fault, similar to the 1984 M_w 6.1 Morgan Hill earthquake. However, the lack of *S* waves at teleseismic distances for the Morgan Hill earthquake and the smaller amplitude of its surface waves as recorded at GTT suggest that the 1911 earthquake had a greater magnitude ($6.3 \geq M_w \geq 6.6$), its direction of rupture propagation was different than the 1984 event, or the data are suspect. Because both GTT and DBN are located along strike to the northwest of the epicenter (Fig. 3), unilateral rupture to the southeast in 1984 (Bakun *et al.*, 1984) and toward the northwest in 1911 might explain some of the amplitude differences between seismograms.

Search for Historical Evidence of 1906 or 1911 Calaveras Slip

To learn if the Calaveras fault slipped in response to the 1906 earthquake, we searched for evidence of surface slip or deformation. We searched for astronomic-azimuth measurements that might have been carried out by the Lick Observatory to align its telescope at Mt. Hamilton, which is located 5–10 km north of the 1911 epicenter. We also looked for cultural offset or geological observations from the contemporary literature, including newspaper accounts of ruptured conduits or offset railways, roads, or fences, and (cadastral) surveying measurements for property boundaries. A Southern Pacific railway line crosses the fault obliquely 2.5 km north of Hollister but no archives of rail repairs from this period exist. The 20 April 1906 edition of the Hollister newspaper reported that "The big water main on Fifth Street

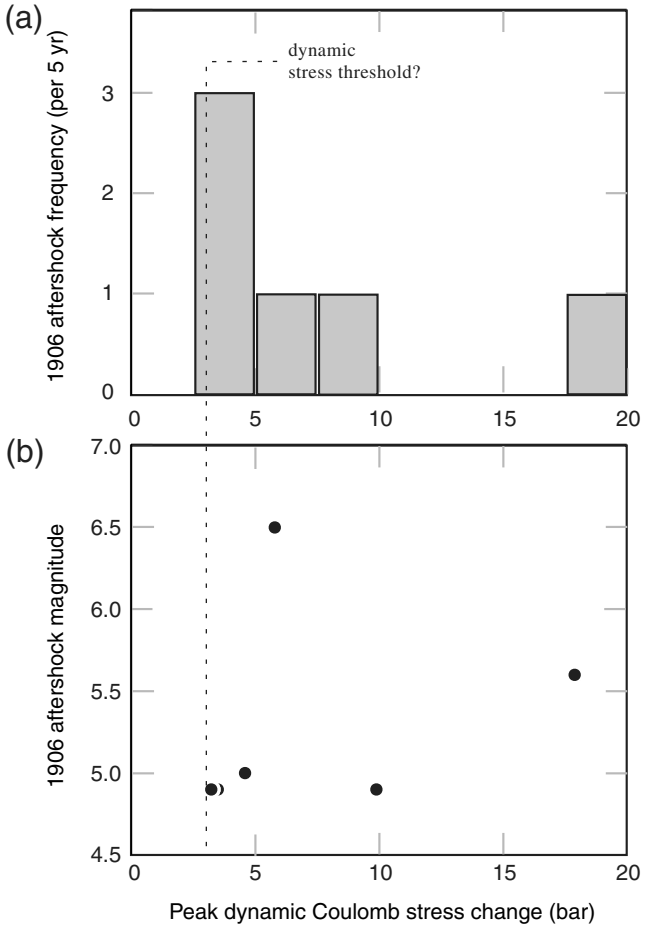

Figure 10. 1906 aftershock (a) frequency and (b) magnitude as a function of calculated peak dynamic Coulomb stress change. 1906 aftershocks from Meltzner and Wald (2003) up through the 1911 event are included; their fault planes are assumed to be parallel to the local strike of the San Andreas fault, with a friction coefficient of 0.6. Because of location uncertainty, the mean stress change within a circle of radius 5 km is used for the calculation. The Song *et al.* (2008) source model for the 1906 earthquake is used. Although no positive correlation is observed in either case, all shocks occurred where the peak dynamic Coulomb stress exceeded 3 bar, perhaps indicative of a threshold for dynamic triggering.

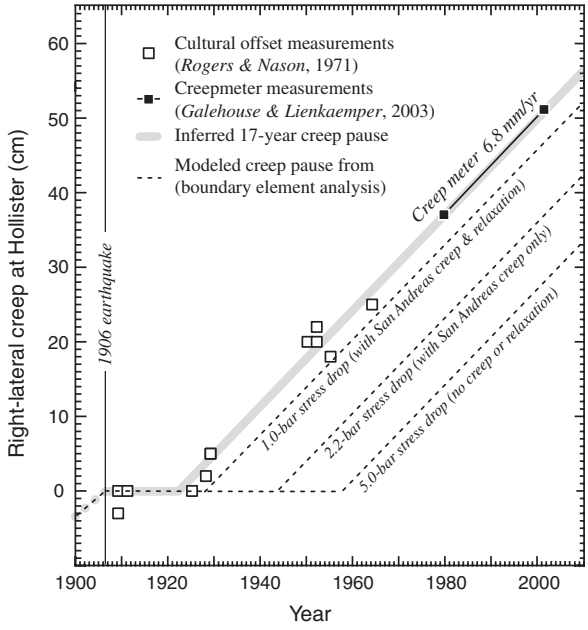

Figure 11. Creep observations (boxes and solid black line) at Hollister since 1910 compared to stress relaxation models. The thick gray line indicates the inferred 17 yr creep pause, and the dashed black lines indicate creep retardation models for the 2–5 bar stress drop in 1906.

was torn heavily apart, and but for the prompt action of the water company, the town would have been without water (The Free Lance, 1906)." The Calaveras fault traverses Fifth Street between Powell and West Streets (Rogers and Nason, 1971), but where on Fifth Street the water main was ruptured was not reported. The water main is likely to have been a buried cast iron pipe and so fault offset is possible but equivocal. E. C. Templeton reported in Oldenbach (1911) that at the time of the 1911 shock, "the earthquake cracked the loose gravels at the side of the stream … At one house near here, the most serious damage was the disconnecting of a water pipe at a windmill" on the Coyote Creek 2 km northeast of Edenvale, near the Calaveras fault. Although this could be associated with coseismic 1911 slip, it is ambiguous.

Post-1906 Creep Retardation at Hollister

Unlike the 1911 site, there are surface slip measurements ~20 km to the southeast at Hollister beginning in 1909 (Fig. 1b). This reveals a likely 17 yr pause in surface creep following the 1906 earthquake, with no change in 1911 (Fig. 11). A boundary-element calculation using the Thatcher *et al.* (1997) model indicates that at Hollister, 0.7 m of left-lateral slip, or a pause in right-lateral creep equivalent to 0.7 m, would have shed the 5 bar of left-lateral stress imposed in 1906 (Fig. 7). If the creeping section of the San Andreas fault extending southeast from Hollister slipped postseismically to relieve the 1906-imposed changes, the Calaveras fault stress drop would reduce to 2.2 bar, and the resulting left-lateral slip needed to relieve the imposed stresses would be 0.5 m (Fig. 7). Given the observed 15 ± 3 mm/yr slip rate at Hollister (6.8 mm/yr of which occurs as surface creep) and the 0.5–0.7 m of backslip, a 33–47 yr pause in Hollister creep would be expected, at least twice as long as the observed pause.

Impact of Viscoelastic Relaxation on Calaveras Earthquakes and Creep

Viscoelastic relaxation speeds the restressing of the Calaveras fault and, thus, could contribute to the shortened creep retardation at Hollister in comparison to purely elastic models. However, viscoelastic recovery does not significantly reload the site of the 1911 earthquake during the 5 yr after the 1906 earthquake. Following a 5 bar 1906 stress

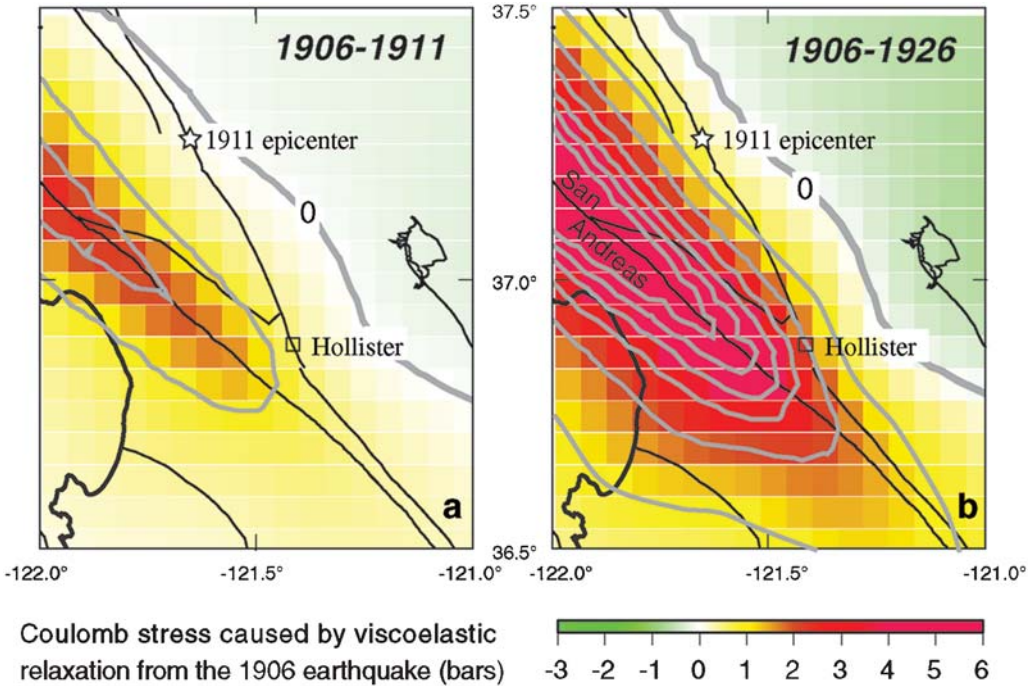

Figure 12. Modeled reloading of fault stress caused by viscoelastic relaxation associated with the 1906 earthquake. (a) At the time of the 1911 earthquake, the Calaveras fault stress has only increased by 0.2 bar. (b) Within several years of the end of the observed creep pause at Hollister, the Calaveras fault has recovered 2.0 bar of Coulomb stress. Long-term or secular stress loading is not included in this calculation.

drop, the stress recovery during the ensuing 5 yr at the 1911 epicenter is calculated to be just 0.15 bar using the model of Pollitz *et al.* (2004) (Fig. 12a). In contrast, at the Hollister site viscoelastic rebound is calculated to reach 1.0 bar by 1916 and 2.0 bar by 1926 (Fig. 12b). This stress recovery approximately matches the observed delay in Hollister creep (Fig. 11).

Other Explanations for the Occurrence of the 1911 Shock

Harris and Simpson (1998) invoked rate/state friction of Dieterich (1994) to explain the occurrence of the 1911 earthquake. They posited that if in the absence of the 1906 earthquake that section of the Calaveras fault would have ruptured in 1908, then the 1906 stress shadow could have delayed the event by only 5 yr. This arises because in rate/state friction theory, a given stress change has a more modest effect in delaying or advancing the rupture late in an earthquake cycle (Dieterich, 1994). While an intriguing hypothesis, it is unfortunately untestable because the unperturbed failure time of the Calaveras fault patch cannot be known. Hori and Kaneda (2001) supposed that because of fault creep, the stressing rate surrounding the locked 1911 patch could be as high as 1–2 bar/yr—much higher than our two independent estimates—in which case, the 1906 stress decrease would have been erased in several years, making the 1911 event more likely. The 17 yr delay at Hollister makes the Hori and Kaneda (2001) explanation for the occurrence of the 1911 earthquake less tenable because the Hollister creep pause should have also been very brief if the stressing rate were in fact as high as 1–2 bar/yr.

Conclusions

First-motion, body-wave, and teleseismic surface-wave analysis for the first time permits a focal mechanism analysis of the 1911 Calaveras earthquake. We find that it was most likely an M_w ~6.5 right-lateral strike-slip event on the Calaveras fault. Our mechanism, location, and magnitude are consistent with assumptions made by Oppenheimer *et al.* (1990), Harris and Simpson (1998), and Bakun (1999) but inconsistent with Jaumé and Sykes (1996), who suggested that it was a reverse mechanism located east of the Calaveras fault, and likely inconsistent with Hori and Kaneda (2001), who proposed a fault stressing rate that is too high to explain the Hollister creep pause. The mechanism and location of the 1911 shock means that it struck on a fault in the stress shadow of the 1906 earthquake and, thus, cannot be easily reconciled with the static Coulomb stress hypothesis.

The 1911 earthquake occurred only about one-quarter of the way through an expected retardation of about 25 yr caused by the 1906 earthquake, and viscoelastic restressing would have only shortened this by a small amount. Thus, the best explanation for the occurrence of the 1911 shock is that it was promoted by the peak dynamic Coulomb stress

imparted by the 1906 earthquake. Nevertheless, there are not enough well-located aftershocks to be confident in this assessment.

We also find that creep retardation occurred at Hollister, just 20 km to the southeast on the Calaveras fault, which also lies in the stress shadow of the 1906 earthquake. The 17 yr creep retardation can be fully explained by the coseismic stress drop, postseismic San Andreas fault creep, and viscoelastic recovery. Thus, the creep retardation provides evidence in support of the static Coulomb hypothesis. In contrast, the San Andreas fault at Hollister is calculated to have experienced a peak dynamic CFF of 6–10 bar; and thus if creep were also driven by dynamic stresses above 3 bar, the creep should have accelerated rather than paused.

Data and Resources

Seismograms used in this study were obtained from individual seismograph stations or published sources listed in the references.

Acknowledgments

We thank reviewers Steve Jaumé and Debi Kilb and David Oppenheimer for comments that greatly improved the manuscript. We also thank Elliot Grunewald, Lee Rosenberg, Willie Lee, John Ebel, and Steve Jaumé for their assistance in locating seismograms and other historical information. We would also like to thank seismograph station managers around the world who maintained and helped us recover the 1911 and 1984 seismograms.

References

Baker, M. R., and D. I. Doser (1988). Joint inversion of regional and teleseismic earthquakes waveforms, *J. Geophys. Res.* **93,** 2037–2045.

Bakun, W. H. (1999). Seismic activity of the San Francisco Bay region, *Bull. Seismol. Soc. Am.* **89,** 764–784.

Bakun, W. H., M. M. Clark, R. S. Cockerham, W. L. Ellsworth, A. G. Lindh, W. H. Prescott, A. F. Shakal, and P. Spudich (1984). The 1984 Morgan Hill, California, earthquake, *Science* **225,** 228–291.

Dieterich, J. (1994). A constitutive law for rate of earthquake production and its application to earthquake clustering, *J. Geophys. Res.* **99,** 2601–2618.

Doser, D. I., and S. R. VanDusen (1996). Source processes of large ($M \geq 6.5$) earthquakes of the southeastern Caribbean (1926–1960), *Pure Appl. Geophys.* **146,** 43–66.

Ellsworth, W. L. (1990). Earthquake history, 1769–1989, in *The San Andreas Fault System, California*, R. E. Wallace (Editor), Chap. 6, *U.S. Geol. Surv. Profess. Pap. 151*, 153–188.

Felzer, K. R., and E. E. Brodsky (2005). Testing the stress shadow hypothesis, *J. Geophys. Res.* **110,** B0SS09, doi 10.1029/2004JB003277.

Felzer, K. R., and T. Cao (2008). The uniform California earthquake rupture forecast version 2 (UCERF 2), in *Appendix H: WGCEP Historical California Earthquake Catalog*, *U.S. Geol. Surv. Open-File Rept. 2007-1437-H*, 127 pp. (http://pubs.usgs.gov/of/2007/1437/h/of2007-1437h.pdf, last accessed March 2009).

Gutenberg, B., and C. F. Richter (1954). *Seismicity of the Earth and Associated Phenomena*, Second Ed. Princeton U Press, Princeton, New Jersey, 310 pp.

Harris, R. A., and R. W. Simpson (1998). Suppression of large earthquakes by stress shadows: A comparison of Coulomb and rate-and-state failure, *J. Geophys. Res.* **103,** 24,439–24,451.

Hori, T., and Y. Kaneda (2001). A simple explanation for the occurrence of the 1911 Morgan Hill earthquake in the stress shadow of the 1906 San Francisco earthquake, *Geophys. Res. Lett.* **28,** 2261–2264, doi 10.1029/2000GL012727.

Jaumé, S. C., and L. R. Sykes (1996). Evolution of moderate seismicity in the San Francisco Bay region, 1950 to 1993: Seismicity changes related to the occurrence of large and great earthquakes, *J. Geophys. Res.* **101,** 765–789.

Kilb, D. (2003). A strong correlation between induced peak dynamic Coulomb stress change from the 1992 *M* 7.3 Landers, California, earthquake and the hypocenter of the 1999 *M* 7.1 Hector Mine, California, earthquake, *J. Geophys. Res.* **108,** 2012, doi 10.1029/2001JB000678.

Kilb, D., J. Gomberg, and P. Bodin (2002). Aftershock triggering by complete Coulomb stress changes, *J. Geophys. Res.* **107,** 2060, doi 10.1029/2001JB000202.

Manaker, D. M., A. J. Michael, and R. Bürgmann (2005). Subsurface structure and kinematics of the Calaveras–Hayward fault stepover from three-dimensional V_P and seismicity, San Francisco Bay region, California, *Bull. Seismol. Soc. Am.* **95,** 446–470.

Meltzner, A. J., and D. J. Wald (2003). Aftershocks and triggered events of the great 1906 California earthquake, *Bull. Seismol. Soc. Am.* **93,** 2160–2186.

Murray, J., and J. Langbein (2006). Slip on the San Andreas fault at Parkfield, California, over two earthquake cycles, and the implications for seismic hazard, *Bull. Seismol. Soc. Am.* **96,** S283–S303.

Oldenbach, F. L. (1911). Notes on the California earthquake of July 1, 1911, *Bull. Seismol. Soc. Am.* **1,** 110–121.

Olsen, K. B. (1994). Simulation of three-dimensional wave propagation in the Salt Lake Basin, *Ph.D. Thesis*, University of Utah.

Oppenheimer, D. H., W. H. Bakun, and A. G. Lindh (1990). Slip partitioning of the Calaveras fault, California, and prospects for future earthquakes, *J. Geophys. Res.* **95,** 8483–8498.

Parsons, T. (2006). Tectonic stressing in California modeled from GPS observations, *J. Geophys. Res.* **111,** B03407, doi 10.1029/2005JB003946.

Pollitz, F., W. H. Bakun, and M. Nyst (2004). A physical model for strain accumulation in the San Francisco Bay region: Stress evolution since 1838, *J. Geophys. Res.* **109,** B11408, doi 10.1029/2004JB003003.

Rogers, T. H., and R. D. Nason (1971). Active displacement on the Calaveras fault zone at Hollister, California, *Bull. Seismol. Soc. Am.* **61,** 399–416.

Segall, P., and Y. Du (1993). How similar were the 1934 and 1966 Parkfield earthquakes?, *J. Geophys. Res.*, **98,** 4527–4538.

Simpson, R. W., and P. A. Reasenberg (1994). Earthquake-induced static-stress changes on central California faults, *U.S. Geol. Surv. Profess. Pap. 1550-F*, 55–89.

Song, S.-G., G. C. Beroza, and P. Segall (2008). A unified source model for the 1906 San Francisco earthquake, *Bull. Seismol. Soc. Am.* **98,** 823–831.

Stein, R. S. (1999). The role of stress transfer in earthquake occurrence, *Nature* **402,** 605–609.

Templeton, E. C. (1911). The central California earthquake of July 1, 1911, *Bull. Seismol. Soc. Am.* **1,** 167–169.

Thatcher, W., G. Marshall, and M. Lisowski (1997). Resolution of fault slip along the 470-km-long rupture of the great 1906 San Francisco earthquake and its implications, *J. Geophys. Res.* **102,** 5353–5367.

The Free Lance (1906). Earthquake! Havoc and destruction wrought in a few seconds; Hollister's loss is $250,000, *Hollister Calif. Newspaper*, **XXIII**, no. 16, 20 April 1906.

Toda, S., and R. S. Stein (2002). Response of the San Andreas fault to the 1983 Coalinga–Nuñez earthquakes: An application of interaction-based probabilities for Parkfield, *J. Geophys. Res.* **107,** 2126, doi 10.1029/2001JB000172.

Toppozada, T. R. (1984). History of earthquake damage in Santa Clara county and comparison of 1911 and 1984 earthquakes, in *The 1984 Morgan Hill, California, Earthquake*, J. H. Bennett and R. W. Sherburne (Editors), **68**, Calif. Div. Mines Geol. Spec. Publ., Sacramento, California, 237–248.

Wald, D. J., H. Kanamori, D. V. Helmberger, and T. H. Heaton (1993). Source study of the 1906 San Francisco earthquake, *Bull. Seismol. Soc. Am.* **83,** 981–1019.

Wells, D. L., and K. J. Coppersmith (1994). New empirical relationships among magnitude, rupture length, rupture width, rupture area, and surface displacement, *Bull. Seismol. Soc. Am.* **84,** 974–1002.

Wills, C. J., R. J. Weldon II, and W. A. Bryant (2008). The uniform California earthquake rupture forcast, version 2 (UCERF 2), in *Appendix A: California Fault Parameters for the National Seismic Hazard Maps and Working Group on California Earthquake Probabilities 2007*, *U.S. Geol. Surv. Open-File Rept. 2007-1437A*, 51 pp. (http://pubs.usgs.gov/of/2007/1437/a/of2007-1437a.pdf, last accessed March 2009).

Wood, H. O. (1912a). On the region of origin of the central Californian earthquakes of July, August, and September, 1911, *Bull. Seismol. Soc. Am.* **2,** 31–39.

Wood, H. O. (1912b). The registration of earthquakes at the Berkeley station from April 1 to September 30, 1911 and at the Lick Observatory station from May 23 to September 30, 1911, *Bull. Seismogr. Stn.*, no. 2, Univ. Calif. Publ., 11–48.

Department of Geological Sciences
University of Texas at El Paso
El Paso, Texas 79968
(D.I.D.)

Department of Geological Sciences
San Diego State University
MC1020
San Diego, California 92182-1020
(K.B.O.)

U.S. Geological Survey
345 Middlefield Road, MS 977
Menlo Park, California 94025
(F.F.P., R.S.S.)

Geological Survey of Japan
Advanced Institute of Science and Technology
Higashi 1-1
Tsukuba 305-8567, Japan
(S.T.)

Manuscript received 21 December 2007